International Journal of Thermofluid Science and Technology (2019)
Volume 6, Issue 3, Paper No. 19060303
https://doi.org/10.36963/IJTST.19060303

Research Article

# The Effects of Thermocapillarity on the Thin Film Flow of MHD UCM Fluid over an Unsteady Elastic Surface with Convective Boundary Conditions

**Hanumesh Vaidya[1], K.V. Prasad[1*], K. Vajravelu[2], Chiu-On Ng[3], S. Nadeem[4], U.B.Vishwanatha[1]**

[1] *Department of Mathematics, VSK University, Vinayaka Nagar, Ballari-583 105, Karnataka, India*
[2] *Department of Mathematics, Department of Mechanical, Materials and Aerospace Engineering, University of Central Florida, Orlando, FL 32816, USA*
[3] *Department of Mechanical Engineering, The University of Hong Kong, Pokfulam, Hong Kong*
[4] *Department of Mathematics, Quaid-i-Azam University, Islamabad, 45320, Pakistan*

Received: 20 June 2019; Received in revised form: 27 November 2019; Accepted: 28 November 2019; Published online 30 November 2019



## Abstract

The study of two-dimensional flow and heat transfer in a liquid film of MHD Upper Convective Maxwell (UCM) fluid over an unsteady elastic stretching sheet subject to velocity slip and convective boundary condition is presented. Thermocapillarity effects are considered. Using suitable similarity transformations, the momentum and thermal energy equations are converted to a set of coupled nonlinear ordinary differential equations. These equations are solved numerically using the Keller-Box method. The velocity and the temperature distributions are presented graphically for different values of the pertinent parameters. The effects of the unsteady parameter on the skin friction, the wall temperature gradient, and the film thickness are tabulated and analyzed. The thermocapillarity parameter has a decreasing effect on the temperature field and the local skin-friction coefficient.

***Keywords*:** Thermocapillarity; Thin film; Velocity slip; UCM Fluid; Marngoni number; Keller box method

## 1. Introduction

In recent years, the investigation of thin-film flows and its rheological properties have pulled in consideration of various scientists as a result of its broad applications in science and Technological ventures. A portion of the applications is; wire coating, fiber coating, reactor fluidization, drawing, and annealing. The learning of flow and heat transfer inside thin-film flows is essential in understanding a few procedures, for example, the coating process, chemical process, polymer process, foodstuff process, and metallurgical processes. The dynamics of films on heated substrates are by and large represented by the main constraints, which form the basis for the formulation of thin films. They are a gravitational force, surface tension,

*Corresponding e-mail: prasadkv2007@gmail.com (K V Prasad).

thermocapillarity (temperature dependence of the surface tension), phase change, as well as the intermolecular forces(See Davis (1987)). The collaboration of these powers regularly results in complex nonlinear conduct shown by the films. Because of the diminishing of the film, as it stretches with the boundary, the nature of the model will be unsteady. Considering these applications, Wang (1990) was the first among the others to ponder Newtonian liquid in a thin liquid film determined by an unsteady stretching surface and obtained similarity solution which satisfied Navier–Stokes equations. Several researchers (Andersson,2000; Dandapat,2003; Wang,2006; Liu, 2008) continued the work of Wang (1990)by taking heat transfer characteristics into account. Dandapat et al. (2007) accomplished a numerical solution for the five-parameter problem and examined the effects of thermocapillarity on the thin film flow in the presence of variable fluid properties. Further, Noor et al. (2010) utilized an analytical technique HAM to analyze MHD flow and heat transfer in a thin liquid film over an unsteady stretching sheet, and Aziz et al. (2011) analyzed the mathematical model of Dandapat B.S,(2007)with inner heating.

All these investigators, however, confined their examinations to the thin liquid film flow of Newtonian fluids. However, many industrial fluids are non-Newtonian in nature or rheological in their flow characteristics and these fluids exhibit dynamic deviation from Newtonian behavior depending upon the flow configuration and/or the rate of deformation. This is maybe because of their extensive variety of utilization, for example, liquid plastics, polymers, suspension, foods, slurries, paints, glues, printing inks, blood, exotic lubricants. Chen (2003), Wang and Pop (2006) and Prasad et al. (2013) studied power-law fluid film over an unsteady stretching sheet. Further, Asghar et al. (2007) considered two thin-film flows of a Sisko fluid on a moving belt. Hayat et al. (2008), Makinde et al. (2009) and Kumaran et al. (2012)analyzed thin film flow of third-grade fluid with different geometry. Kumaran et al. (2012) presented an exact solution for the thin film flow of a third-grade fluid on an inclined plane, which was the corrected version of the earlier published solution. Further, Vajravelu et al. (2012) explored the effects of temperature-dependent thermal conductivity on an unsteady flow and heat transfer in a thin liquid film of Ostwald–de Waele fluid over a horizontal permeable stretching surface.

There are few non-Newtonian models which are known to be precise only for weakly elastic fluids subject to gradually varying flows and to violate certain rules of thermodynamics, namely, viscoelastic and Walters' models. Concerning the polymer industry, the outcomes detailed in the above works are constrained. In this manner, the outcomes which are vital for industry, broader viscoelastic liquid models, for example, upper convicted Maxwell model (UCM fluid) or Oldroyd B model should be invoked. Numerous researchers have done extensive work on Upper Convective Maxwell fluid with different geometry with the boundary conditions prescribed at the sheet and on the fluid at infinity. (See Hayat et al. (2006), Vajravelu et al. (2011), Sabeel et al. (2017), Saleem et al. (2017), and Nadeem et al. (2017)). To the authors' best knowledge, the combined study of the flow and heat transfer in a thin liquid film of an electrically conducting UCM fluid combined with velocity slip and convective boundary condition on a horizontal elastic sheet has not been carried out. In the present paper, we investigate the effect of the transverse magnetic field on thermocapillary driven thin film flow and heat transfer of an incompressible non-Newtonian UCM fluid induced by an accelerating unsteady elastic sheet with convective boundary condition. The presence of thermocapillarity couples the hydrodynamic and the thermal boundary layer problems. In addition to this, many non–Newtonian complex fluids find wall slip such as emulsions, suspensions, foams, and polymer

solutions; therefore, in a thin film flow of non-Newtonian UCM fluid, the effect of velocity slip is prominent. Consequently, we examine considering the impacts of velocity slip on the thin film flow of UCM fluid(See Prasad et al. (2018), Vaidya et al. (2018)).

The governing nonlinear coupled system of equations for flow and heat transfer have been reduced to a nonlinear coupled ordinary differential equation by using a suitable similarity transformation and is solved via an efficient second-order finite difference scheme known as the Keller-box method(Keller,1992; Vajravelu,2014; Prasad,2015,2016). The obtained numerical results are analyzed graphically. The analysis reveals that the thin film flow of UCM fluid is appreciably influenced by the physical parameters. It is expected that the results obtained will not only provide useful information for industrial applications but also complement the existing literature.

## 2. MathematicalModeling of the Problem

Consider an unsteady, laminar, viscous flow and heat transfer in an electrically conducting UCM thin liquid film with convective boundary condition on a horizontal sheet which issues from a slot (See Fig.1). The fluid motion along the x-axis within the thin liquid film arises due to the stretching of an elastic sheet, whereas the *y*-axis perpendicular to it. Intermolecular forces come into effect because the fluid layer considered is not so thin, and hence, the buoyancy force is neglected. The flow region is exposed under a uniform transverse magnetic field $\vec{B}_0 = (0, B_0, 0)$ with low magnetic Reynolds number and the imposition of such magnetic field stabilizes the boundary layer flow.

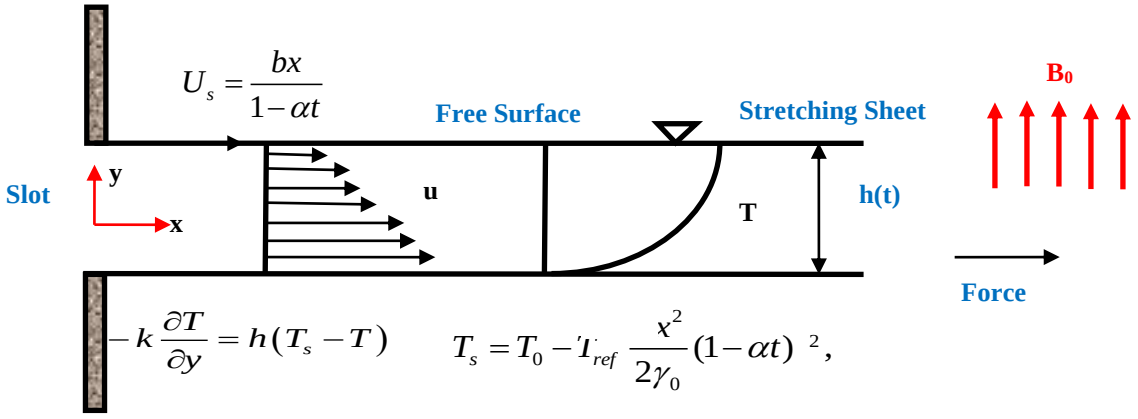


**Fig. 1: Schematic representation of the physical model and coordinate system.**

The Navier-Stokes equations with prescribed nonlinear boundary conditions will be solved numerically under the following assumptions

- The continuous elastic sheet is stretched by applying a force in the positive *x*-direction with a surface velocity $U_s = \frac{bx}{1-\alpha t}$ which is fixed at the origin and the prescribed

surface temperature be $T_s = T_0 - T_{ref}\frac{b\,x^2}{2\gamma_0}(1-\alpha t)^{-\frac{3}{2}}$, where $b>0$ **and** $\alpha>0$ are constants with dimension (time)$^{-1}$ and $bx(1-\alpha t)^{-1}$. Here, $T_0$ is the temperature at the origin and $T_{ref}$ is the reference temperature such that $0 \le T_{ref} \le T_0$ , the above expressions are valid for time $t < \alpha^{-1}$.

- The fluid motion within the thin film of uniform thickness $h(t)$ is caused solely by the linear stretching of an elastic sheet.
- The surface-tension $\sigma$ considered to vary linearly with temperature as $\sigma = \sigma_0\left(1-\gamma_1\left(T-T_0\right)\right)$ here $T$ is the temperature, $\sigma_0$ is surface tension at the slit temperature $T_0$ and $\gamma_1 = \left(\sigma_0\left(\partial\sigma/\partial T\right)_{T=T_0}\right)^{-1}$ is the positive temperature coefficient of the surface tension (Dandpat et al. (2007)).
- Negligible interfacial shear due to air is assumed; however, the variation of $\sigma$ along the surface is $\frac{\partial\sigma}{\partial x} = \frac{\partial\sigma}{\partial T}\frac{\partial T}{\partial x}$ and the interfacial flow generated due to this is the major concern in this study. In spite of this, a balance between the viscous shear stress $\tau = -\mu\,\partial u/\partial y$, and the thermal stress prevails which is of the form $\mu\frac{\partial u}{\partial y} = \frac{\partial\sigma}{\partial x}$.

Under these assumptions, the governing equations along with the boundary layer approximations with an unsteady state can be written as

$$\frac{\partial u}{\partial x} + \frac{\partial \mathrm{v}}{\partial y} = 0, \tag{1}$$

$$\frac{\partial u}{\partial t} + u\frac{\partial u}{\partial x} + \mathrm{v}\frac{\partial u}{\partial y} = \frac{1}{\rho}\left(\frac{\partial \tau_{xx}}{\partial x} + \frac{\partial \tau_{xy}}{\partial y}\right) - \frac{\sigma_1 B_0^2}{\rho}\left(u + \lambda_1 \mathrm{v}\frac{\partial u}{\partial y}\right), \tag{2}$$

$$\frac{\partial \mathrm{v}}{\partial t} + u\frac{\partial \mathrm{v}}{\partial x} + \mathrm{v}\frac{\partial \mathrm{v}}{\partial y} = \frac{1}{\rho}\left(\frac{\partial \tau_{xx}}{\partial x} + \frac{\partial \tau_{yy}}{\partial y}\right), \tag{3}$$

$$\frac{\partial T}{\partial t} + u\frac{\partial T}{\partial x} + \mathrm{v}\frac{\partial T}{\partial y} = \alpha_0\left(\frac{\partial^2 T}{\partial x^2} + \frac{\partial^2 T}{\partial y^2}\right), \tag{4}$$

where $u$ and v are the velocity components along with the $x$ and $y$ directions respectively, $\rho$ is the density, $\tau_{xy}$ is the shear stress, $\sigma_1$ is the electrical conductivity, $B_0^{\,2}(t) = B_0^2\left(1-\alpha t\right)^{-1}$ is the special form of the uniform magnetic field(see Prasad et al. (2013)) and $\alpha_0$ is the thermal diffusivity. In the present model, we consider $\partial u/\partial y \le 0$ throughout the entire boundary layer and the fluid obeys the upper convected Maxwell model. For a Maxwell fluid, we have

$$\tau_{ij} + \lambda_1\left(\frac{D}{Dt}\tau_{ij} - L_{jk}\tau_{ik} - L_{ik}\tau_{kj}\right) = 2\delta\, d_{ij}, \tag{5}$$

where $\tau_{ij}$ is the extra tensor, $d_{ij}$ is the deformation rate tensor, $\delta$ is the coefficient of viscosity and $\lambda_1$ is the relaxation time of the period and $L_{ij}$ is the velocity gradient tensor. For an incompressible fluid obeying upper convected Maxwell model, the momentum equation and the energy equation can be simplified using the usual boundary layer theory approximations (Wang (1990), Andersson et al. (2000), Sadeghy et al. (2006))as

$$\frac{\partial u}{\partial t}+u\frac{\partial u}{\partial x}+\mathrm{v}\frac{\partial u}{\partial y}+\lambda_1\left(u^2\frac{\partial^2 u}{\partial x^2}+\mathrm{v}^2\frac{\partial^2 u}{\partial y^2}+2u\mathrm{v}\frac{\partial^2 u}{\partial x\partial y}\right)=\nu\frac{\partial^2 u}{\partial y^2}-\frac{\sigma_1 B_0^2}{\rho}\left(u+\lambda_1\mathrm{v}\frac{\partial u}{\partial y}\right), \tag{6}$$

$$\frac{\partial T}{\partial t}+u\frac{\partial T}{\partial x}+\mathrm{v}\frac{\partial T}{\partial y}=\alpha_0\frac{\partial^2 T}{\partial y^2} \tag{7}$$

The boundary conditions for a thin fluid film with velocity partial slip are

$$u=U_s+N\gamma_s(t)\frac{\partial u}{\partial y},\quad \mathrm{v}=\mathrm{v}_s\quad ,-k_s\frac{\partial T}{\partial y}=h_s(t)(T_s-T)\qquad \text{at}\quad y=0, \tag{8}$$

$$\mu\frac{\partial u}{\partial y}=\frac{\partial\sigma}{\partial x}\quad \text{at}\ \ y\to h(t), \tag{9}$$

$$\frac{\partial T}{\partial y}=0\qquad \text{at}\ \ y\to h(t), \tag{10}$$

$$\mathrm{v}=\frac{dh}{dt}\qquad \text{at}\ \ y\to h(t), \tag{11}$$

Here $N$ the velocity slip factor, $k_s$ is the thermal conductivity of the fluid, $h_s$ is the convective heat transfer coefficient, and $T_s$ is the convective fluid temperature. Introducing similarity transformation for non-dimensional variables $f,\theta$ and $\eta$ as (see for details Wang (2006) and Dandapat et al. (2007)

$$\psi=(\nu b)^{\frac{1}{2}}x(1-\alpha t)^{\frac{-1}{2}}\beta f(\eta), \tag{12}$$

$$T=T_0-T_{ref}\left(\frac{b\,x^2}{2\nu}\right)(1-\alpha t)^{-\frac{3}{2}}\theta(\eta)\qquad \text{and} \tag{13}$$

$$\eta=\left(\frac{b}{\nu}\right)^{\frac{1}{2}}(1-\alpha t)^{\frac{-1}{2}}\beta^{-1}y\ . \tag{14}$$

here $\beta>0$ is the film thickness, the actual film thickness with $\eta=1$ **at** $y=h$(at free surface), form Eq. (15) we have $h(t)=\beta\left(\frac{\nu}{b}\right)^{\frac{1}{2}}(1-\alpha t)^{\frac{1}{2}}$ and the rate-of-change of the fillm thickness is $\frac{dh}{dt}=-\frac{1}{2}\alpha\beta\left(\frac{b}{\nu}\right)^{-\frac{1}{2}}(1-\alpha t)^{\frac{-1}{2}}$ . The stream function $\psi(x,y,t)$ is defined by $u=\psi_y=bx(1-\alpha t)^{-1}f'(\eta)$ and $\mathrm{v}=-\psi_x=-(b\nu)^{1/2}(1-\alpha t)^{-1/2}\beta f(\eta)$ , which automatically

satisfies mass conservation Eq. (1). In terms of these new non-dimensional variables, the equations (6) and (7) together with the boundary conditions (8) to (11) become

$$\frac{1}{\beta^2} f''' - \left( f'^2 - f\, f'' \right) - S\left( \frac{\eta}{2} f'' + f' \right) + \lambda \left( 2 f f f'' - f^2 f''' \right) - Mn\left( f' + \lambda f\, f'' \right) = 0 \tag{15}$$

$$\mathrm{Pr}^{-1} \theta'' + \beta^2 \left( f\theta' - f' 2\theta \right) - \frac{S\beta^2}{2} \left( 3\theta + \eta \theta' \right) = 0 \tag{16}$$

and

$$f(0) = 0, \;\; f'(0) = 1 + k_0 \frac{1}{\beta} f''(0), \;\; \theta'(0) = -\beta B_i \left( 1 - \theta(0) \right), \tag{17}$$

$$f''(\beta) - M\theta(\beta) = 0, \;\; f(\beta) = \frac{S\beta}{2}, \; \theta'(\beta) = 0. \tag{18}$$

where $\theta = \dfrac{(T - T_0)}{(T_s - T_0)}$ and prime denotes the differentiation with respect to $\eta$, $\beta$ is the dimensionless film thickness which depends only on time *t*. The special form for the velocity slip factor $\gamma_s = \gamma_s (1 - \alpha t)^{1/2}$ and heat transfer coefficient $h_s(t) = h_s (1 - \alpha t)^{1/2}$ are chosen to obtain the similarity solution. The parameters $S$ are the dimensionless measure of the unsteadiness, Pr is the Prandtl number, $\lambda$ is the Maxwell parameter, $M$ is the thermocapillarity parameter (surface tension gradient)emerged during the course of similarity analysis which is the replica of Marangoni number, frequently observed in the analysis of thermocapillary driven flows , $k_0$ is the slip parameter, *Mn* is the magnetic parameter, and $B_i$ is the Biot number which are defined as

$$S = \frac{\alpha}{b}, \;\; \mathrm{Pr} = \frac{\nu}{\alpha}, \;\; \lambda = \lambda_1 b, \;\; M = \frac{\delta \sigma_0 T_{ref}}{\mu \sqrt{b\nu}}, \;\; Mn = \frac{\sigma B_0^2}{\rho b}, \;\; k_0 = N \gamma_s \sqrt{\frac{b}{\nu}}, \;\; B_i = \frac{h_s}{k_s} \sqrt{\frac{\nu}{b}}.$$

For a Newtonian fluid, the present mathematical model reduces to Wang (2006) when $Mn = M = k_0 = B_i = \lambda = 0$. The quantities of engineering interest such as the local skin friction coefficient $C_{fx}$, and the local Nusselt number $Nu_x$ can be written as

$$C_{fx} = \frac{\tau_w}{\rho U_s^2}, \tag{19}$$

where the wall skin friction $\tau_w$ is given by

$$\tau_w = \mu \left( \frac{\partial u}{\partial y} \right)_{y=0} - \lambda_1 \left( 2u\mathbf{v} \frac{\partial u}{\partial x} + \mathbf{v}^2 \frac{\partial u}{\partial y} \right)_{y=0} \tag{20}$$

using variables (20), we get

$$C_{fx} = \left\{ f''(0) - \beta \left[ f^2(0) f''(0) - 2 f(0) f'^2(0) \right] \right\} Re_x^{-1/2} \text{ and} \tag{21}$$

$$Nu_x = -\frac{x}{T_{ref}}\left(\frac{\partial T}{\partial y}\right)_{y=0} = \frac{1}{2}(1-\alpha t)^{-1/2}\, Re_x^{3/2}\, \theta'(0). \tag{22}$$

where $Re_x = \dfrac{bx^2}{\nu(1-\alpha t)}$ is the local Reynolds number. It is clear from equations (21) and(22)that $C_{fx}$ decreases linearly with the distance from the slit, whereas $Nu_x$ increases as $x^3$ .

# 3.Numerical procedure

The equations (15) and (16) are highly coupled nonlinear fifth-order ordinary differential equations with the third order in $f(\eta)$ and second order in $\theta(\eta)$. These equations subject to the boundary conditions (17) and (18) constitute a two-point boundary value problem on the interval [0, $\beta$ ]. The set of equations with the appropriate boundary conditions are solved numerically via an efficient numerical method with a second-order finite difference scheme known as the Keller-box method (see for details Keller(1992), Vajravelu and Prasad(2014, 2015, 2016)). In order to validate the obtained results; we compare numerical results with the available results in the literature reported by Wang (2006), Noor et al. (2010), Aziz et al. (2011) and Vajravelu et al. (2012) which is shown in Table 1, and are found to be in excellent agreement.

# 4. Results and Discussion

Exact analytical solutions for the complete set of equations (15) and (16) which is highly coupled and nonlinear ordinary differential equations is not possible. Employing the numerical scheme, the system of equations is solved for several sets of values of the unsteady parameter $S$ , the Maxwell parameter $\lambda$ , the thermocapillarity parameter $M$ , the slip parameter $k_0$ , the magnetic parameter $Mn$, the Prandtl number $\Pr$ and the Biot number $B_i$. Graphically presented numerical results in Figs. 2–7 give a clear insight into the physical model; the variations in horizontal velocity profile $f'(\eta)$, transverse velocity profile $f(\eta)$, the temperature profile $\theta(\eta)$ for different values of the physical parameters are reported in these figures. The solution of thermocapillary driven thin film flow exists only for $0 \le S \le 2$ and $S = 2$ is the critical value for a Newtonian fluid (See for details Wang (2006)). When $S \to 0(\beta \to \infty)$ we obtain the analytical solution for an infinitely thick fluid layer; whereas the limiting case of $S \to 2(\beta \to 0)$ represents a liquid film of infinitesimal thickness. However, it is difficult to perform these calculations for the limiting case of $\beta \to \infty$. The computed numerical values for the skin friction $f''(0)$, the Nusselt number $\theta'(0)$ and dimensionless film thickness $\beta$ are recorded in Table 2.

Figures.2(a) through 2(c) depict the effects of S on $f(\eta), f'(\eta)$ and $\theta(\eta)$ for $k_0 = 0$ and $k_0 \neq 0$. It is clear from these profiles that $f(\eta)$ increase while $f'(\eta)$ decreases monotonically as the distance increase from the slit. The increase in $S$ and $k_0$ leads to a rise in all the three profiles $f(\eta), f'(\eta)$ and $\theta(\eta)$, that is, the rise in the friction and the flow velocity is registered due to a rise in S on the surface. When friction increases, the area of the stretching

surface in contact with the flow increases, therefore generated heat from the friction on the surface is transferred to the flow and thereby enhances the velocity and thermal boundary layer thickness. A similar phenomenon may be observed in the case of $f''(\eta)$ and $\theta'(\eta)$ (See table 2 for details). The effect of $S$ on $f'(\eta)$ and $\theta(\eta)$ for different values of $Mn$ and $\lambda$ can be observed from Figs.3(a) to 3(c) respectively. As $S, Mn$ and $\lambda$ increases, the velocity and temperature profile increase and hence increase in the momentum and thermal boundary layer thickness is observed and the velocity distribution becomes linear for higher values of $S$. It is worth mentioning; an increase in the velocity and skin friction for large values of $Mn$ is marginal whereas in the case of temperature and wall temperature gradient it is large (See table 2). This nature of $f'(\eta)$ and $f''(0)$ may be attributed to Lorentz force thereby. Meanwhile, the temperature of the flow rises appreciably with the rise in $Mn$. Fig. 4(a) and Fig. 4(b) elucidate the effect of $S$ on $f(\eta)$ in the presence and absence of the Maxwell parameter. As $S$ increases, the transverse velocity profile increases in both cases. Fig.5 shows $\theta(\eta)$ and $\theta'(\eta)$ profiles for various values $S$ along with varying values of $B_i$. It is evident from Fig 5. that decreasing the temperature and the local skin-friction coefficient. As $B_i$ increases, the internal thermal resistance of the plate is larger than the boundary layer thermal resistance. Hence, an increase in $B_i$ tends to increase in the fluid temperature efficiently. Moreover, $\theta'(\eta)$ converges to 0 along the sheet satisfying the boundary conditions. The nondimensional temperature and skin friction for different values of $S$ and $M$ is plotted in Fig. 6. Increase in the thermocapillarity number $M$ (surface tension gradient), the temperature consistently cools down and decreases. Hence, the fluid layer just below the free surface is dragged along by the top layer due to viscous shear and also it shows that the temperature decreases with an increase in the thermocapillarity parameter. The decline of the flow temperature reduces the vibrating force in the fluid molecules. From mass conservation law, when the force in the flow direction decreases, the skin friction also decreases. Thus surface-tension gradients generate an interfacial flow that, through viscous drag, oppose the shear-driven motion due to the stretching sheet. This is even true for increasing values of $S$ .Fig.7 demonstrate the effect of increasing values of $S$ and Pr on $\theta(\eta)$. Augmented Pr results in a decrease in the temperature distribution and it tends to zero as the distance increases from the elastic sheet. For large Pr, the thermal boundary layer is contained within the lower part of the thin liquid film and the temperature gradients vanish adjacent to the free surface. Hence, the thermal boundary layer thickness decreases for large Pr and is exactly reversed in the case of $S$ .

In Table 2 we present the results for $f''(0)$, $\theta'(0)$ and $\beta$ corresponding to different values of the physical parameters. For increasing values of $S$, skin friction, Nusselt number increases, whereas the values of the film thickness decrease, and this is true even in the case of $Mn$ also. Increase in $M$ results in a decrease in $f''(0)$ and $\theta'(0)$ and increase in $\beta$. For increasing values of Pr, the Nusselt number decreases.

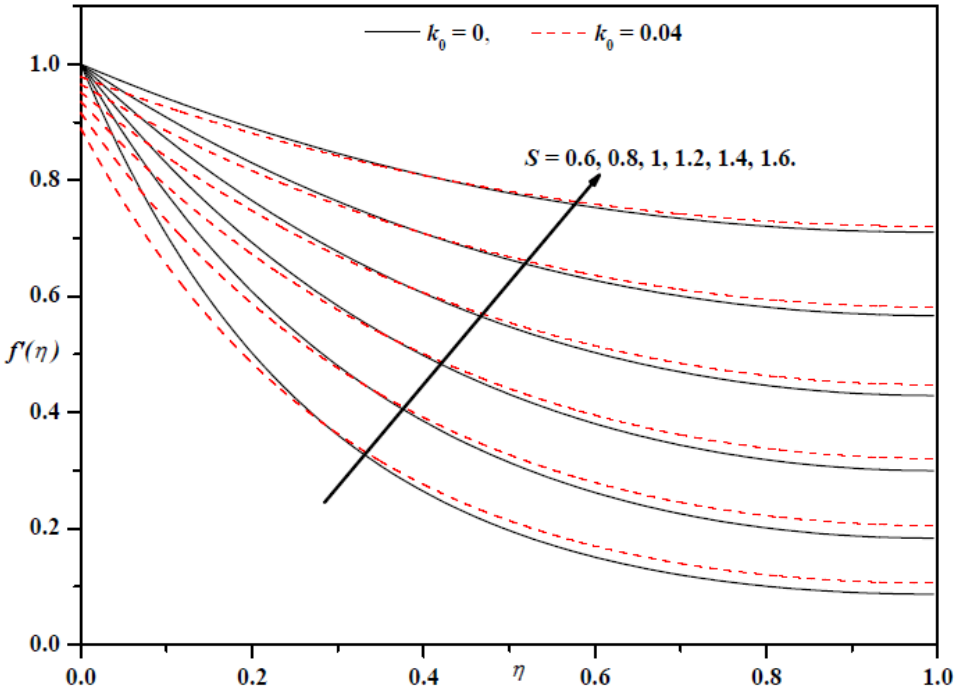


**Fig.2(a) : Horizontal velocity profiles for different values of $k_0$ and $S$ with $B_i = 0.5$, $Mn = 0.2$, $\lambda = 0.2$, $\mathrm{Pr} = 1$, $M = 0$.**

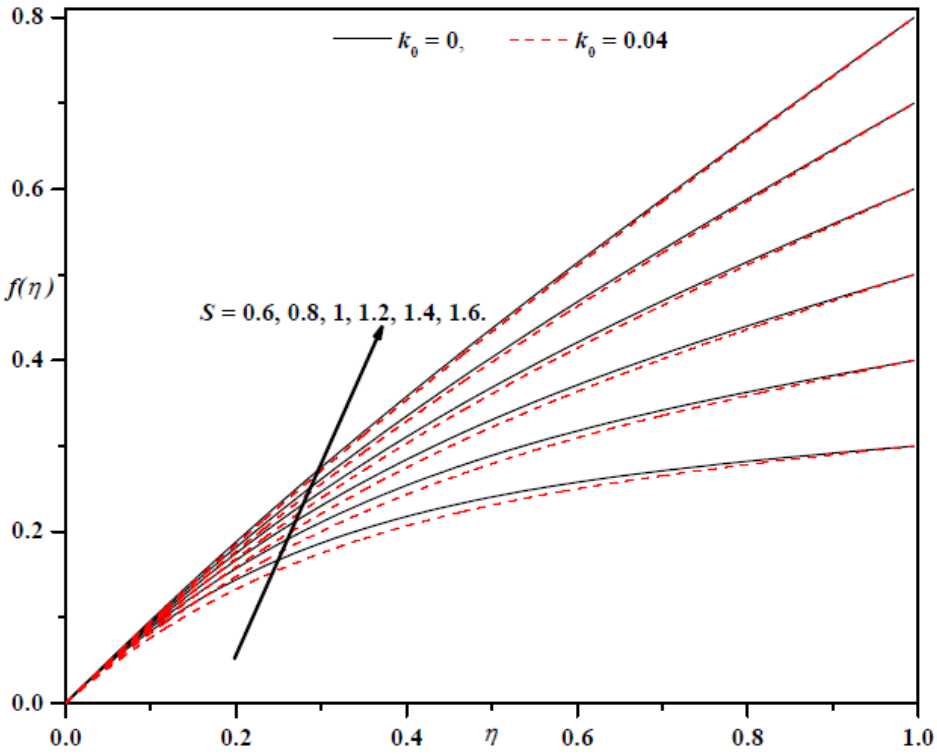


**Fig.2(b): Transverse velocity profiles for different values of $k_0$ and $S$ with $B_i = 0.5$, $Mn = 0.2$, $\lambda = 0.2$, $\mathrm{Pr} = 1$, $M = 0$.**

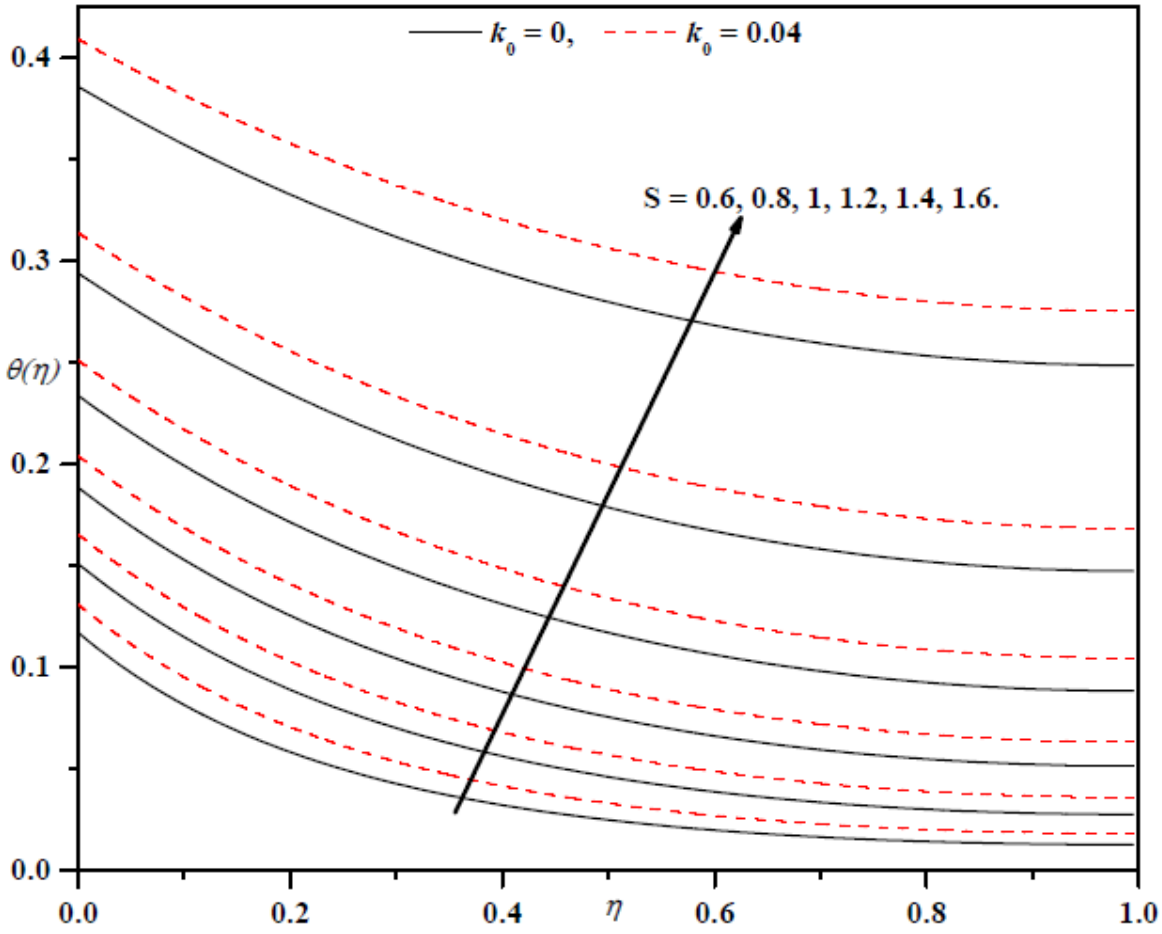


**Fig.2(c): Temperature profiles for different values of $k_0$ and $S$ with Pr = 1, $\lambda = 0.2$, $M = 0$, $Mn = 0.5$, $B_i = 0.5$.**

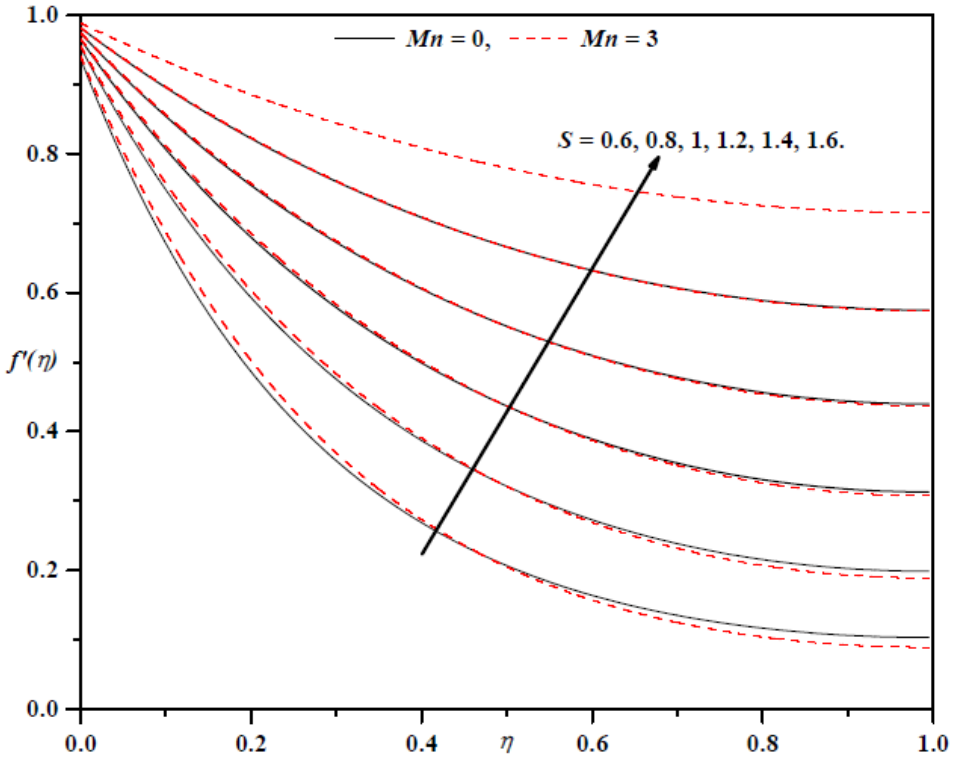


**Fig.3(a): Horizontal velocity profiles for different values of *Mn* and *S* with $B_i = 0.5$, $k_0 = 0.02$, $\lambda = 0.2$, Pr = 1, $M = 0$.**

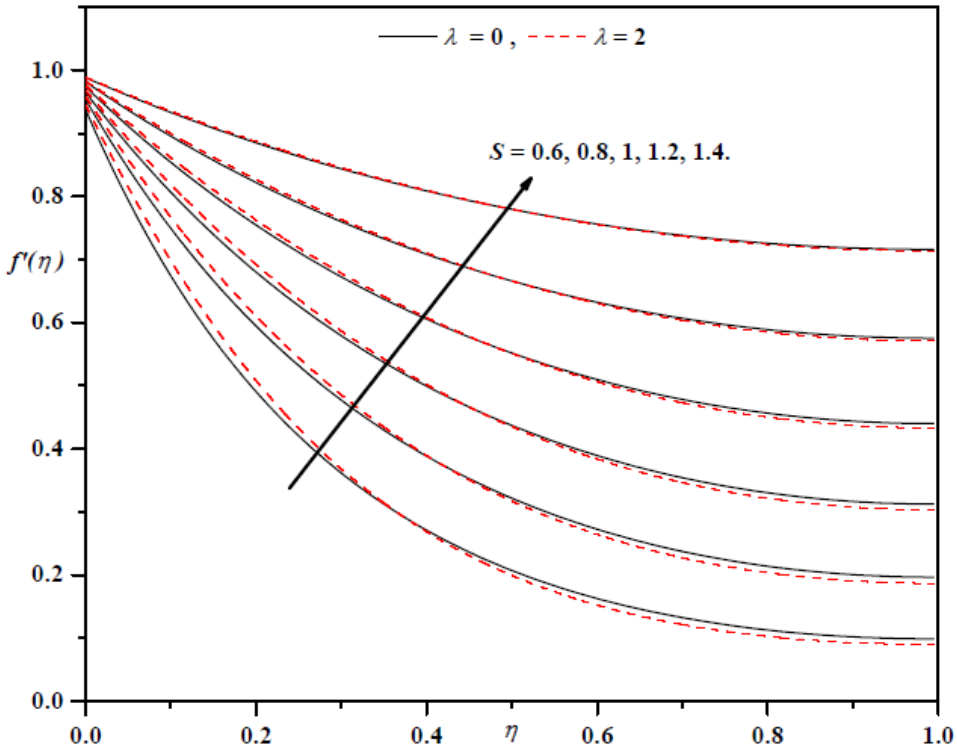


**Fig.3(b): Horizontal velocity profiles for different values of λ and $S$ with $B_i = 0.5$, $k_0 = 0.02$, $Mn = 0.5$, Pr = 1, $M = 0$.**

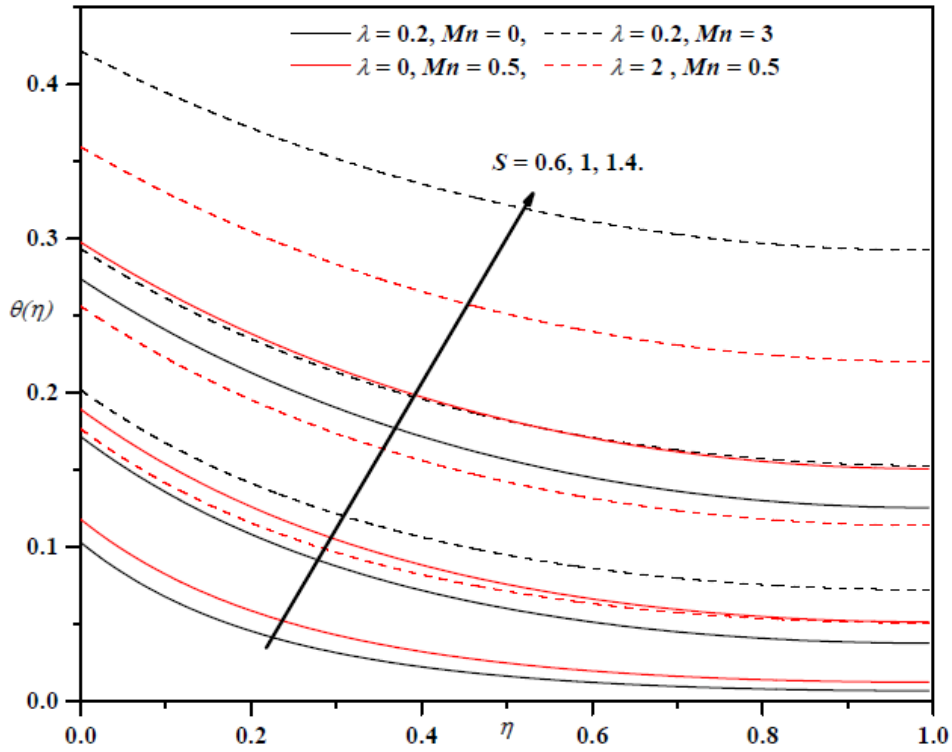


**Fig.3(c): Temperature profiles for different values of $Mn$ , $\lambda$ and $S$ with $k_0 = 0.02$, Pr = 1, $M = 0$, $B_i = 0.5$.**

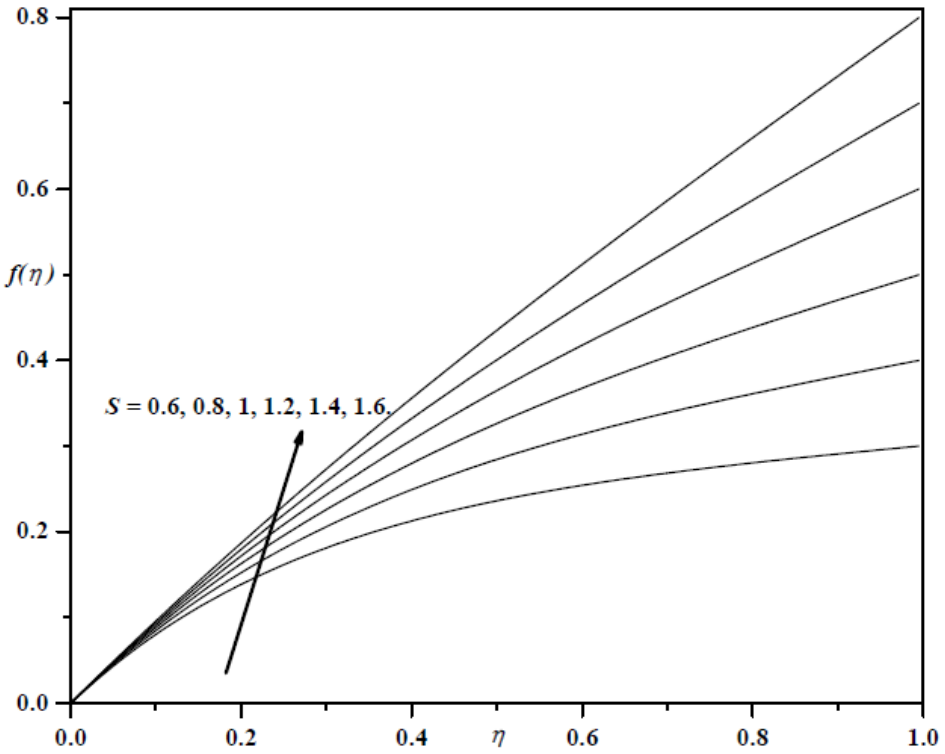


**Fig.4(a): Transverse velocity profiles for different values of $S$ with $B_i = 0.5$, $Mn = 0.2$, $k_0 = 0.02$, Pr = 1, $\lambda = 0.4$, $M = 0$.**

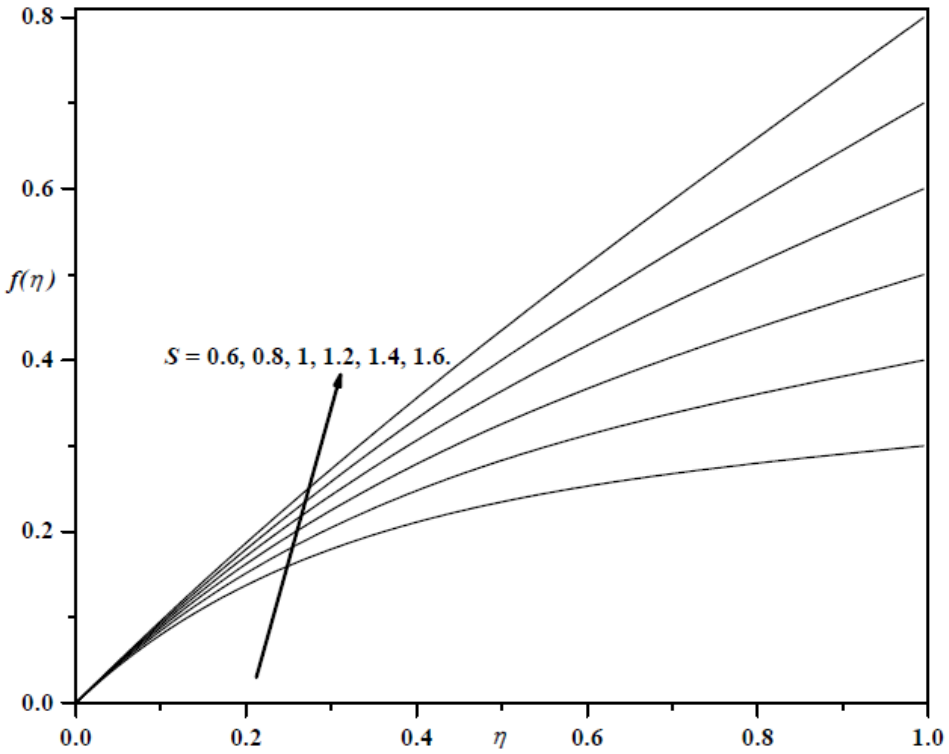


**Fig.4(b): Transverse velocity profiles for different values of $S$ with $\lambda = 0$, $B_i = 0.5$, $Mn = 0.2$, $k_0 = 0.02$, Pr = 1, $M = 0$.**

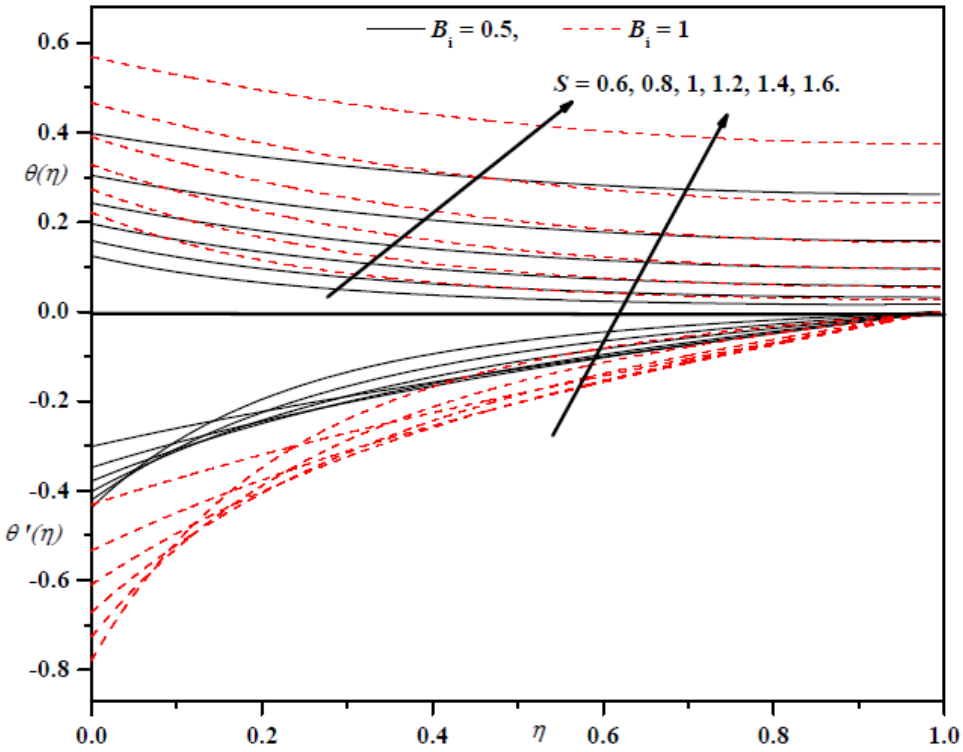


**Fig.5: Temperature profiles for different values of $B_i$ and $S$ with $k_0 = 0.02$, Pr = 1, $\lambda = 0.2$, $M = 0$ , $Mn = 0.5$.**

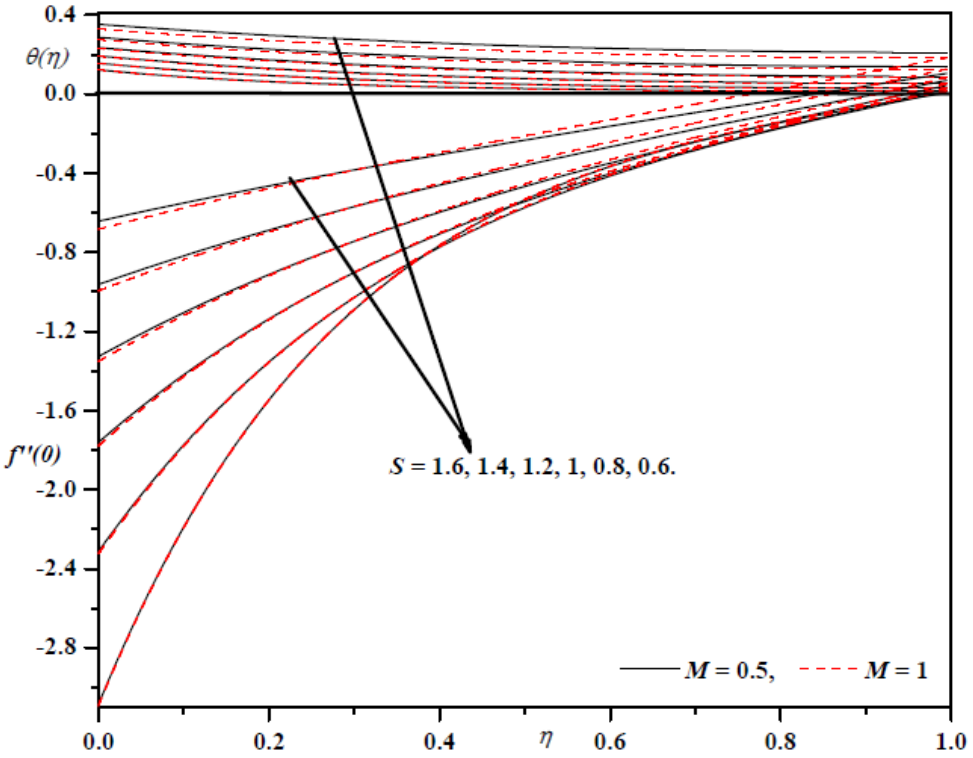


**Fig.6: Temperature and Skin friction profiles for different values of $M$ and $S$ with $k_0 = 0.02$, Pr = 1, $\lambda = 0.2$, $B_i = 0.5$, Mn = 0.5.**

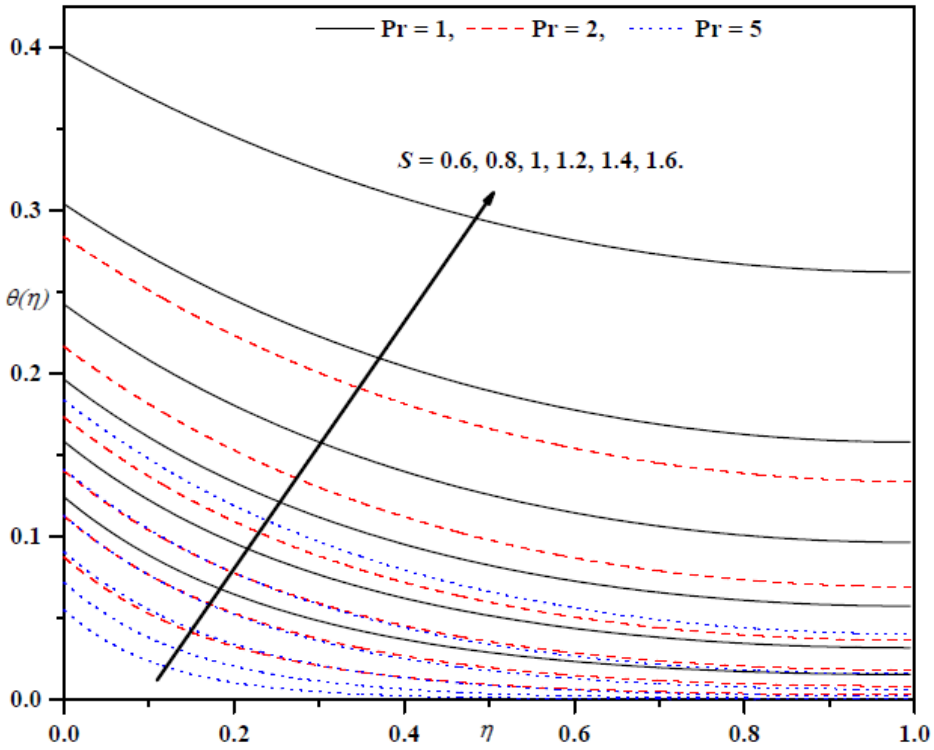


**Fig.7: Temperature profiles for different values of Pr and $S$ with $k_o = 0.02$, $\lambda = 0.2$, $M = 0$, $Mn = 0.5$, $B_i = 0.5$.**

# 5. Conclusion

The obtained numerical results via Keller-box method and its analysis lead to some of the following conclusions:

- The velocity and the temperature increase with an increase in the unsteady parameter and the slip parameter. This phenomenon is true even with the applied magnetic field and the Maxwell parameter.
- The increasing thermocapillarity parameter decreases the temperature, the local skin-friction coefficient and the local Nusselt number.
- The temperature profile broadens when the unsteady parameter increases.
- An increase in the Biot number leads to an increase in the thermal boundary layer thickness.
- The increasing value of the Prandtl number reduces the dimensionless temperature within the fluid film.

# Acknowledgments

**The authors appreciate the constructive comments of the reviewers which led to definite improvement in the paper.**

# References

Andersson, H. I., Aarseh, J. B. and Dandapat, B. S., "Heat Transfer in a Liquid Film on anUnsteady Stretching Surface," International Journal of Heat and Mass Transfer, 43, 69-74 (2000).

Aziz RC, Hasim I, Almari AK. Thin film flow and heat transfer on an unsteady stretching sheet with internal heating. Meccanica; 46:349–57(2011).

Chen, C. H. Heat transfer in a power-law fluid film over an unsteady stretching sheet. Heat and Mass Transfer,39, 791–796 (2003).

Davis, S.H., Thermocapillary instabilities, Annu. Rev. Fluid Mech., 19 (1987), 403–435.

Dandapat, B. S., Santra, B. and Anderson, H. I., "Thermocapillarity in a Liquid Film on Unsteady Stretching Surface," International Journal of Heat and Mass Transfer, 46, 3009-3015 (2003).

Dandapat B.S,B.Santra, K.Vajravelu, The effect of variable fluid properties and thermocapillarity on the flow of a thin film on an unsteady stretching sheet, InternationalJournal of Heat and Mass Transfer, -96 (2007).

Hayat, T., Ellahi, R., Mahomed, F.M.: Exact solutions for thin film flow of a third-grade fluid down an inclined plane. Chaos Solitons Fractals 38, 1336–1341 (2008).

Hanumesh Vaidya, Manjunatha Gudekote, Rajashekhar Choudhari, Prasad K.V., Role of slip and heat transfer on peristaltic transport of Herschel-Bulkley fluid through an elastic tube, (2018), Multidiscipline Modeling in Materials and Structures, DOI: 10.1108/MMMS-11-2017-0144.

H.B. Keller, Numerical Methods for Two-point Boundary Value Problems, Dover Publ, New York (1992).

KV Prasad, K Vajravelu, PS Datti, BT Raju, MHD Flow,and Heat Transfer in a Power-law Liquid Film at a Porous Surface in the Presence of Thermal Radiation, Journal ofApplied Fluid Mechanics, 6(3), 385-395, (2013).

K Vajravelu, KV Prasad, Chiu-On Ng, Unsteady flow and heat transfer in a thin film of Ostwald–de Waele liquid over a stretching surface, CNSNS,17(11),4163-4173(2012).

K. Vajravelu, K. V. Prasad, A. Sujatha, Convection heat transfer in a Maxwell fluid at a non-isothermal surface, Cent. Eur. J. Phys. 9(3),807-815(2011)

K. V. Prasad, K. Vajravelu, Hanumesh Vaidya, M. M. Rashidi, and Neelufer .Z.Basha, Flow and Heat Transfer of a Casson Liquid over a Vertical Stretching Surface: Optimal Solution, American Journal of Heat and Mass Transfer, (2018) Vol. 5 No. 1 pp. 1-22. doi:10.7726/ajhmt.2018.100.

K. Vajravelu and K.V. Prasad, Keller-box method and its application, HEP and Walter De Gruyter GmbH, Berlin/Boston (2014).

K. V. Prasad, H. Vaidya,and K. Vajravelu, MHD Mixed Convection Heat Transfer in a Vertical Channel with Temperature-Dependent Transport Properties,***J**ournal of **A**pplied **F**luid **M**echanics*, Vol. 8, No. 4, pp. 693-701, (2015).

K. V. Prasad, K. Vajravelu, and H. Vaidya, MHD Casson Nanofluid Flow and Heat Transfer at a Stretching Sheet with Variable Thickness, Journal of Nanofluids, Vol.5(3), (2016), pp. 423-435(13).

K. V. Prasad, H. Vaidya,K. Vajravelu, M. M. Rashidi, Effects of variable fluid properties on MHD flow and heat transfer over a stretching sheet with variable thickness, Journal of Mechanics, 33(4), 501-512. doi:10.1017/jmech.2016.101.

Liu I. C., Anderson, H.I. Heat transfer in a liquid film on an unsteady stretching sheet.International Journal of Thermal Sciences, 47(6): 766-772(2008).

Makinde, O.D.: Thermal criticality for a reactive gravity-driven thin film flow of a third-grade fluid with adiabatic free surface down an inclined plane. Appl. Math. Mech.30, 373–380 (2009)

M Sabeel. Khana, M. Hammad, S. Batool, and H. Kaneez Investigation of MHD effects and heat transfer for the upper-convected Maxwell (UCM-M) micropolar fluid with Joule heating and thermal radiation using a hyperbolic heat flux equation, Eur. Phys. J. Plus 132: 158 (2017).

Noor N. F. M., Abdulaziz O.,and Hasim I. MHD flow and heat transfer in a thin liquid film on a unsteady stretching sheet by the Homotopy analysis method.International Journal for Numerical Methods in Fluids, 63(3): 357-373 (2010).

S. Asghar, T. Hayat, A. H. Kara, Exact solutions of thin film flows, Nonlinear Dyn,50:229–233(2007).

S.Saleem, M.Awais, S.Nadeem, N.Sandeep, M.T.Mustafa, Theoretical analysis of upper-convected Maxwell fluid flow with Cattaneo–Christov heat flux model, Chinese Journal of Physics, 55(4), 1615-1625, (2017).

Sohail Nadeem, Shafiq Ahmad, Noor Muhammad, M.T. Mustafa, Chemically reactive species inthe flow of a Maxwell fluid, Results in Physics, 7 ,2607–2613(2017).

T. Hayat Z. Abbas, M. Sajid Series solution for the upper-convected Maxwell fluid over aporous stretching plate, Physics Letters A 358 396–403(2006).

V. Kumaran, R. Tamizharasi, J. H. Merkin, K. Vajravelu, On thin film flow of a third-grade fluid down an inclined plane, Arch Appl Mech ,82:261–266(2012).

Wang CY. Liquid film on an unsteady stretching surface. Quart Appl Math; 48:601–10 (1990).

Wang, C., Analytic Solutions for a Liquid Thin Film on an Unsteady Stretching Surface, Heat and Mass Transfer, 42, 759-766(2006).

Wang, C. and Pop, I. Analysis of the flow of a power-law fluid film on an unsteady stretching surface by means of homotopy analysis method. Journal of Non-Newtonian Fluid Mechanics, 138, 161–172 (2006).

**Table1: Variation of skin friction $f''(0)$ and dimensionless film thickness $\beta$ with the unsteady parameter $S$ for Newtonian fluid when** $\Pr = 1.0,\ Mn = M = B_i = k_0 = \lambda = 0.0.$

| $S$ | Wang (2006) | | Noor et al. (2010) | | Aziz et al. (2011) | | Vajravelu et al.(2012) | | Present work | |
|---|---|---|---|---|---|---|---|---|---|---|
| | $f''(0)$ | $\beta$ | $f''(0)$ | $\beta$ | $f''(0)$ | $\beta$ | $f''(0)$ | $\beta$ | $f''(0)$ | $\beta$ |
| 0.8 | -2.680940 | 2.151990 | -2.680940 | 2.15199 | - 2.680943 | 2.151994 | -2.677546 | 2.149956 | -2.68094 | 2.15199 |
| 1.0 | -1.972380 | 1.543620 | -1.972380 | 1.54362 | - 1.972384 | 1.54362 | -1.967298 | 1.540905 | -1.97238 | 1.54362 |

| | | | | | | | | | | |
|---|---|---|---|---|---|---|---|---|---|---|
| 1.2 | -1.442631 | 1.127780 | -1.442631 | 1.12778 | - 1.442625 | 1.127780 | -1.435752 | 1.124422 | -1.44263 | 1.12778 |
| 1.4 | -1.012784 | 0.821032 | -1.012784 | 0.821032 | - 1.012784 | 0.821032 | -1.003991 | 0.816898 | -1.012780 | 0.821032 |
| 1.6 | -0.642397 | 0.567173 | -0.642397 | 0.576173 | - 0.642397 | 0.576173 | -0.631578 | 0.570868 | -0.631597 | 0.576173 |
| 1.8 | - 0.309137 | 0.356389 | −0.309137 | 0.356389 | - 0.309137 | 0.356389 | -0.296197 | 0.348569 | -0.296197 | 0.348569 |

**Table 2: Variation of skin friction $f''(0)$, wall-temperature gradient $\theta'(0)$ and dimensionless film thickness $\beta$, for different values of the physical parameters.**

| Pr | $B_i$ | $M$ | $Mn$ | $\lambda$ | $S$ | $f''(0)$ | $\theta'(0)$ | $\beta$ | $f''(0)$ | $\theta'(0)$ | $\beta$ | $f''(0)$ | $\theta'(0)$ | $\beta$ |
|---|---|---|---|---|---|---|---|---|---|---|---|---|---|---|
| | | | | | | $k_0 = 0.0$ | | | $k_0 = 0.02$ | | | $k_0 = 0.04$ | | |
| 1.0 | 0.5 | 0.0 | 0.5 | 0.2 | 0.6 | -3.501704 | 0.116937 | 2.440094 | -3.075872 | 0.124248 | 2.329543 | -2.754911 | 0.130856 | 2.237056 |
| | | | | | 0.8 | -2.550409 | 0.150815 | 1.735566 | -2.298145 | 0.158328 | 1.666025 | -2.097146 | 0.165275 | 1.606015 |
| | | | | | 1.0 | -1.901519 | 0.188370 | 1.283763 | -1.740643 | 0.196373 | 1.236551 | -1.607706 | 0.203892 | 1.195033 |
| | | | | | 1.2 | -1.403382 | 0.233623 | 0.962834 | -1.298230 | 0.242467 | 0.929741 | -1.209076 | 0.250868 | 0.900248 |
| | | | | | 1.4 | -0.989572 | 0.293908 | 0.716298 | -0.922168 | 0.304048 | 0.693019 | -0.863933 | 0.313736 | 0.672060 |
| | | | | | 1.6 | -0.626387 | 0.385783 | 0.510999 | -0.586813 | 0.397697 | 0.495156 | -0.552139 | 0.409058 | 0.480777 |
| Pr | $M$ | $Mn$ | $k_0$ | $\lambda$ | $S$ | $B_i = 0.05$ | | | $B_i = 0.5$ | | | $B_i = 1.0$ | | |
| 1.0 | 0.0 | 0.5 | 0.02 | 0.2 | 0.6 | -3.075872 | 0.002829 | 2.329543 | -3.075872 | 0.124248 | 2.329543 | -3.075872 | 0.221033 | 2.329543 |
| | | | | | 0.8 | -2.298145 | 0.003748 | 1.666025 | -2.298145 | 0.158328 | 1.666025 | -2.298145 | 0.273374 | 1.666025 |
| | | | | | 1.0 | -1.740643 | 0.004863 | 1.236551 | -1.740643 | 0.196373 | 1.236551 | -1.740643 | 0.328281 | 1.236551 |
| | | | | | 1.2 | -1.298230 | 0.006361 | 0.929741 | -1.298230 | 0.242467 | 0.929741 | -1.298230 | 0.390299 | 0.929741 |
| | | | | | 1.4 | -0.922168 | 0.008662 | 0.693019 | -0.922168 | 0.304048 | 0.693019 | -0.922168 | 0.466314 | 0.693019 |
| | | | | | 1.6 | -0.586813 | 0.013034 | 0.495156 | -0.586813 | 0.397697 | 0.495156 | -0.586813 | 0.569074 | 0.495156 |
| Pr | $B_i$ | $Mn$ | $k_0$ | $\lambda$ | $S$ | $M = 0.0$ | | | $M = 0.5$ | | | $M = 1.0$ | | |
| 1.0 | 0.5 | 0.5 | 0.02 | 0.2 | 0.6 | -3.075872 | 0.124248 | 2.329543 | -3.083758 | 0.123904 | 2.336536 | -3.091433 | 0.123572 | 2.343338 |
| | | | | | 0.8 | -2.298145 | 0.158328 | 1.666025 | -2.311112 | 0.157321 | 1.677409 | -2.323454 | 0.156379 | 1.688218 |
| | | | | | 1.0 | -1.740643 | 0.196373 | 1.236551 | -1.760187 | 0.193752 | 1.254099 | -1.778170 | 0.191427 | 1.270129 |
| | | | | | 1.2 | -1.298230 | 0.242467 | 0.929741 | -1.326416 | 0.235911 | 0.956349 | -1.351055 | 0.230588 | 0.979207 |
| | | | | | 1.4 | -0.922168 | 0.304048 | 0.693019 | -0.961877 | 0.287520 | 0.733681 | -0.994023 | 0.275898 | 0.765363 |
| | | | | | 1.6 | -0.586813 | 0.397697 | 0.495156 | -0.642114 | 0.353881 | 0.559421 | -0.682100 | -0.329523 | 0.602214 |
| Pr | $B_i$ | $M$ | $k_0$ | $\lambda$ | $S$ | $Mn = 0.0$ | | | $Mn = 1.0$ | | | $Mn = 3.0$ | | |
| 1.0 | 0.5 | 0.0 | 0.02 | 0.2 | 0.6 | -3.170049 | 0.102874 | 2.812084 | -3.028628 | 0.142551 | 2.035747 | -2.956964 | 0.201827 | 1.462821 |
| | | | | | 0.8 | -2.344776 | 0.135143 | 1.956784 | -2.271871 | 0.178735 | 1.476131 | -2.227871 | 0.245962 | 1.083291 |
| | | | | | 1.0 | -1.762500 | 0.171460 | 1.420195 | -1.727302 | 0.218744 | 1.109762 | -1.703130 | 0.293237 | 0.832449 |
| | | | | | 1.2 | -1.307791 | 0.215314 | 1.048795 | -1.292031 | 0.267119 | 0.843805 | -1.280031 | 0.349150 | 0.646222 |
| | | | | | 1.4 | -0.925892 | 0.273743 | 0.770557 | -0.919631 | 0.331551 | 0.634994 | -0.914433 | 0.421513 | 0.495588 |

| Pr | $B_i$ | $M$ | $k_0$ | $Mn$ | $S$ | $\lambda = 0.0$ | | | $\lambda = 0.4$ | | | $\lambda = 2.0$ | | |
|---|---|---|---|---|---|---|---|---|---|---|---|---|---|---|
| 1.0 | 0.5 | 0.0 | 0.02 | 0.5 | 0.6 | -3.142838 | 0.117812 | 2.457346 | -3.018183 | 0.130558 | 2.217216 | -2.752479 | 0.176543 | 1.653901 |
| | | | | | 0.8 | -2.339503 | 0.151366 | 1.744182 | -2.261882 | 0.165173 | 1.596136 | -2.085332 | 0.215580 | 1.227034 |
| | | | | | 1.0 | -1.765215 | 0.189221 | 1.284270 | -1.718646 | 0.203427 | 1.193070 | -1.604011 | 0.255993 | 0.949362 |
| | | | | | 1.2 | -1.311908 | 0.235424 | 0.957920 | -1.285711 | 0.249428 | 0.903565 | -1.215292 | 0.301744 | 0.747050 |
| | | | | | 1.4 | -0.928956 | 0.297505 | 0.708430 | -0.915812 | 0.310518 | 0.678424 | -0.876994 | 0.359350 | 0.584958 |
| | | | | | 1.6 | -0.589496 | 0.392319 | 0.502306 | -0.584244 | 0.403012 | 0.488256 | -0.567120 | 0.443218 | 0.440760 |
| $\lambda$ | $B_i$ | $M$ | $k_0$ | $Mn$ | $S$ | $\Pr = 1.0$ | | | $\Pr = 2.0$ | | | $\Pr = 5.0$ | | |
| 0.2 | 0.5 | 0.0 | 0.02 | 0.5 | 0.6 | -3.075872 | 0.124248 | 2.329543 | -3.075872 | 0.087421 | 2.329543 | -3.075872 | 0.055059 | 2.329543 |
| | | | | | 0.8 | -2.298145 | 0.158328 | 1.666025 | -2.298145 | 0.112518 | 1.666025 | -2.298145 | 0.071858 | 1.666025 |
| | | | | | 1.0 | -1.740643 | 0.196373 | 1.236551 | -1.740643 | 0.140227 | 1.236551 | -1.740643 | 0.090607 | 1.236551 |
| | | | | | 1.2 | -1.298230 | 0.242467 | 0.929741 | -1.298230 | 0.173132 | 0.929741 | -1.298230 | 0.112753 | 0.929741 |
| | | | | | 1.4 | -0.922168 | 0.304048 | 0.693019 | -0.922168 | 0.216504 | 0.693019 | -0.922168 | 0.141183 | 0.693019 |
| | | | | | 1.6 | -0.586813 | 0.397697 | 0.495156 | -0.586813 | 0.283969 | 0.495156 | -0.586813 | 0.183726 | 0.495156 |

3